JOURNAL OF MATERIALS SCIENCE 28 (1993) 3783–3788

Influence of annealing on the mechanical properties of compocast Al(Mg)–Al_2O_3 particulate composite

P. K. GHOSH, S. RAY*
*Department of Metallurgical Engineering, and *Department of Mechanical and Industrial Engineering, University of Roorkee, Roorkee 247 667, India*

The annealing of cast Al(Mg)–Al_2O_3 particulate composite at temperatures of 673, 723 and 773 K for varying periods of time from 1–5 h resulted in reduction of strength and hardness similar to that occurring in cast Al–Mg alloy, due to homogenization. However, the ductility of the composite increased on annealing, contrary to that observed in cast Al–Mg alloy, presumably because the solution of the eutectic in the composite causes magnesium diffusion to the alumina particles resulting in further reaction to form magnesium aluminate and does not increase the magnesium level of its primary phase, as occurs in Al–Mg alloy.

1. Introduction

The compocast Al(Mg)–Al_2O_3 particulate composite has received wide attention due to its good specific strength at ambient [1–3] and elevated [3, 4] temperatures. The mechanical properties of metal–ceramic composites are, to a great extent, governed by their intimate contact and interfacial bonding [5, 6], which facilitates the transfer of load from the matrix to the reinforcing components. In Al(Mg) –Al_2O_3 composite produced by the compocasting process, a reacted layer consisting of magnesium aluminate ($MgAl_2O_4$), has been found to form at the alumina–matrix interface [6, 7] which results in wetting of alumina by molten aluminium alloys. During investigation [6] carried out on the heat treatment of cast Al(Mg)–Al_2O_3 composites it has been observed that the reacted layer is stable and grows further with increasing annealing time and temperature. During annealing of compocast Al(Mg)–Al_2O_3 particulate composite, the matrix also changes considerably, resulting in a decrease in its hardness [6]. Thus, the heat treatment of these composites affects the overall mechanical properties through changes in the matrix and particle–matrix interface. The present study aims to gain an understanding of the influence of heat treatment on the mechanical properties of cast aluminium alloy–alumina particulate composite. The changes in the mechanical properties of the cast Al–Mg alloy have been investigated for reference and comparison.

2. Experimental procedure

The Al(Mg)–Al_2O_3 particulate composite was prepared by the compocasting process. In this process, preheated (1072 K) alumina powders having a broad size range of about 45–212 μm, was added to the vortex formed at the surface of the vigorously stirred partially solid melt freshly innoculated with magnesium, and held at a temperature of 900 K. The stirring speed was kept fixed at 16 rev. s^{-1}. The stirring speed was measured using a strobometer and the holding temperature was measured by placing a chromel–alumel thermocouple at a depth of 15–20 mm inside the melt. The slurry containing alumina particles was stirred for about 300 s and then it was poured into a permanent steel mould of size $25 \times 30 \times 300\ mm^3$ through the bottom of the crucible. Immediately after pouring, the mould was quenched with the help of a water spray. Al–Mg alloy having a similar magnesium content to that of the particulate composite, was also prepared by the addition of magnesium in molten aluminium.

A number of samples from the cast ingot of composite were annealed for different periods of time varying from 1–5 h at temperatures of 673, 723, and 773 K. Similarly, the samples collected from the cast Al–Mg alloy were annealed at the same temperatures of 723, 773 and 823 K, and for the same periods of time. The metallographic studies were carried out under a scanning electron microscope and the thickness of the reacted layer formed at the particle–matrix interface in different annealed specimens of composite was measured under an optical microscope with the help of a microscale having a least count of 0.5 μm. The Vicker's hardness of the matrix of as-cast and annealed specimens of the composite and the Al–Mg alloy was measured at a load of 5 kg.

The tensile specimens, as schematically shown in Fig. 1, were machined from the composites and the cast Al–Mg alloy, and were annealed as described earlier. The alumina and porosity content of each tensile specimen of the composite were determined by

0022–2461 © *1993 Chapman & Hall*

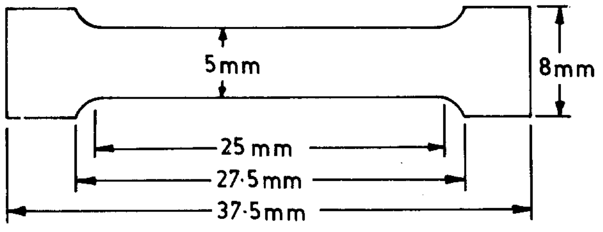

Figure 1 Schematic diagram of the tensile specimen.

combining the observed area fraction of dark spots in the matrix estimated by point counting, and the measured density [8, 9]. The porosity content of tensile specimens of the base alloy was also determined by the weight loss method. The tensile tests were carried out with a Monsanto tensometer at ambient temperature. The elongation of the specimens fractured under tensile loading was estimated at a gauge length of 25 mm. The fracture surface of the tensile specimens, especially those from the composites, was examined under scanning electron microscope to understand the fracture behaviour.

Samples of the as-cast and annealed composites were studied using X-ray diffractometry (XRD) to identify the phases formed in the composites. The X-ray diffraction study was carried out with CuK_α radiation, in a Philips diffractometer (model PW 1140/90), within an angular range of 2θ from 5°–120°.

3. Results

The magnesium contents of Al(Mg)–Al_2O_3 particulate composite and the Al–Mg alloy synthesized for this investigation are estimated as 3.8 and 4.5 wt %, respectively.

The interplanar spacing, d, obtained from the X-ray diffraction analysis of the as-cast and annealed (723 K, 5 h) composites are listed in Table I. A comparison with the ASTM chart reveals the presence of magnesium aluminate ($MgAl_2O_4$) in both the as-cast and annealed composites, as well as the primary phase and α-Al_2O_3. The existence of $MgAl_2O_4$ is established by the peaks corresponding to d-values of 2.8029 and 0.9324 where there is no interference from the other phases present. However, in the composite, no significant response indicating the presence of MgO was seen. The absence of any diffraction line corresponding to Mg_5Al_2 of the eutectic formed due to segregation of the solute is due to its low amount being below the detection level.

The optical micrographs of the composite as-cast and annealed at 773 K for 1 h, are shown in Fig. 2a and b, respectively. These micrographs show that the matrices of the composite are homogenized during annealing, as is also observed in the micrographs of the Al–Mg alloy.

The scanning electron micrographs of the as-cast composite and those annealed at 723 K for 3 h and 673 K for 5 h are shown in Fig. 3a–c, respectively, and these micrographs reveal the influence of heat treatment on the growth of the reacted layer at the particle–matrix interface. Fig. 3a shows that in the as-cast composite, the reacted layer at the particle–matrix interface is sometimes quite non-uniform in thickness. However, during annealing, a further growth of the reacted layer results in a more or less uniform thickness around the particle, as shown in Fig. 3b. The micrograph of the as-cast composite shown in Fig. 3a reveals the presence of microcracks sometimes observed within the reacted layer, as marked by the arrow, and also at the boundary between the unreacted alumina particle and the reacted layer,

TABLE I X-ray diffraction analysis of the composite

Line no.	$\sin\theta$	d (nm)	$(h\,k\,l)$	Phase
1	0.2748	0.280 29	(2 2 0)	$MgAl_2O_4$
2	0.3297	0.233 62	(2 2 2) (1 1 1)	$MgAl_2O_4$ α-Al
3	0.3806	0.202 38	(4 0 0)	$MgAl_2O_4$
4	0.5365	0.143 57	(2 0 0)	α-Al
5	0.5471	0.140 78	(1 2 4)	α-Al_2O_3
6	0.6289	0.122 47	(3 1 1)	α-Al
7	0.6570	0.117 24	(4 4 4) (3 0 6)	$MgAl_2O_4$ α-Al_2O_3
8	0.7584	0.101 56	(4 0 0) (8 0 0) (4 0 2)	α-Al $MgAl_2O_4$ α-Al_2O_3
9	0.8261	0.093 24	(7 5 1)	$MgAl_2O_4$
10	0.8476	0.090 87	(3 2 4) (4 2 0) (8 4 0)	α-Al_2O_3 α-Al $MgAl_2O_4$

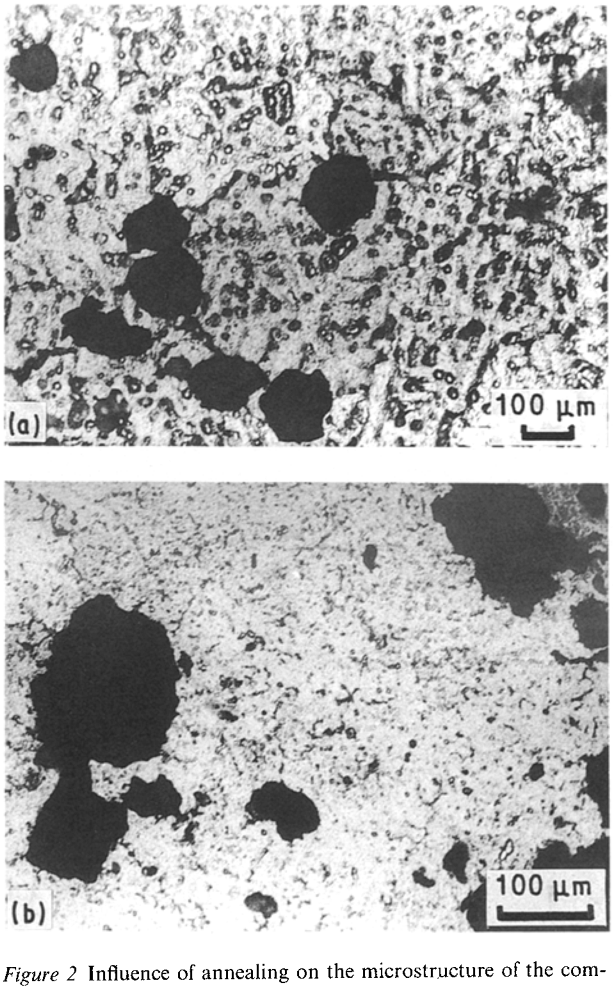

Figure 2 Influence of annealing on the microstructure of the composites; (a) as-cast, and (b) annealed at 773 K for 1 h.

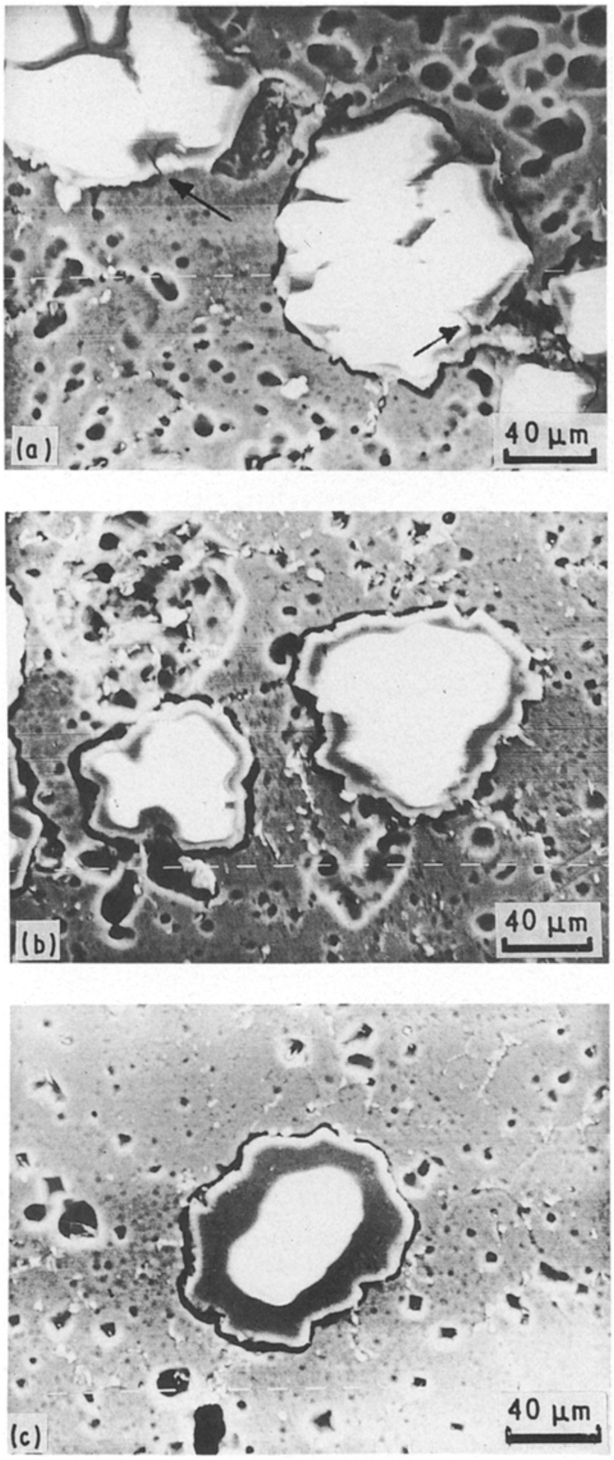

Figure 3 Scanning electron micrographs typically showing the influence of annealing on the reacted layer at the particle–matrix interface: (a) as cast, (b) annealed at 673 K for 5 h and (c) annealed at 723 K for 3 h.

but it has not been observed in the annealed composites despite growth of a comparatively thick reacted layer at the particle–matrix interface.

The alumina and the porosity content of the tensile specimens tested for the mechanical properties of the composites were estimated as 14.0 ± 1.5 and 6.0 ± 1.5 vol %, respectively. The porosity content of the tensile specimens of Al–Mg alloy was estimated to be 2.7 ± 0.6 vol %, in spite of similar casting practice.

The influence of annealing on the matrix hardness of the composite and the Al–Mg alloy are shown in Figs 4 and 5, respectively. The figures show that for a given annealing time of 1 h, the increase in annealing temperature from 673 K to 773 K for the composite and 700 K to 823 K for the Al–Mg alloy, decreases the hardness of the alloy and the matrix of the composite. The increase in extent of annealing also reduces the scattering in distribution of hardness (Fig. 4) in the matrix. At given annealing temperatures of 673 and 723 K for the composite and of 723 and 773 K for the Al–Mg alloy, the influence of annealing time on hardness is as shown in Figs 4 and 5, respectively. The figures show that the increase in annealing time decreases the hardness of the matrix of the composite and that of the Al–Mg alloy.

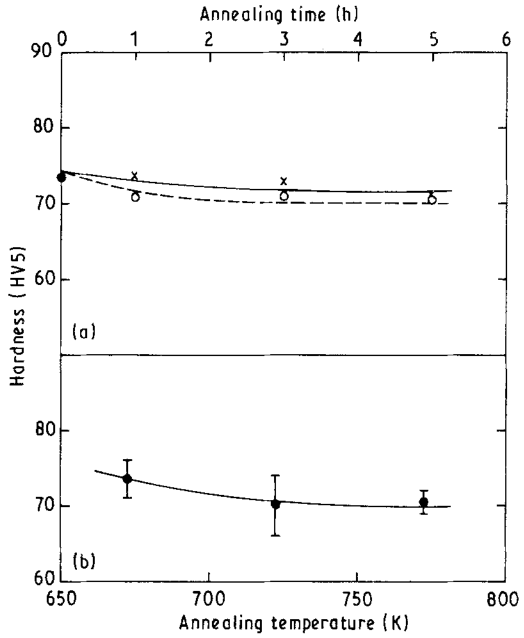

Figure 4 Effect of (a) time and (b) temperature of annealing on the matrix hardness of the composite. (a) (×) 673 K, (o) 723 K, (b) annealing time 1 h.

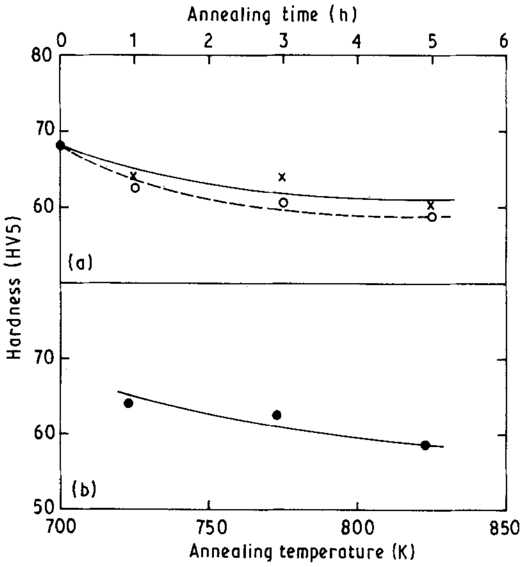

Figure 5 Effect of (a) time and (b) temperature of annealing on the matrix hardness of the Al–Mg alloy. (a) (×) 723 K, (O) 773 K, (b) annealing time 1 h.

At the two different annealing temperatures of 723 and 773 K, the influence of annealing time on the ultimate tensile strength (UTS), σ_u, and elongation of the Al–Mg alloy is as shown in Fig. 6. The figure shows that at a given annealing temperature, the increase in annealing time reduces both the ultimate tensile strength and elongation of the alloy. The figure also shows that at a given annealing time, the ultimate tensile strength and elongation of the alloy are always lower at higher annealing temperature. This behaviour is further evident in Fig. 7 where, at a given annealing time of 1 h, the variation in ultimate tensile strength and elongation are shown with the increase in annealing temperature from 723 K to 823 K.

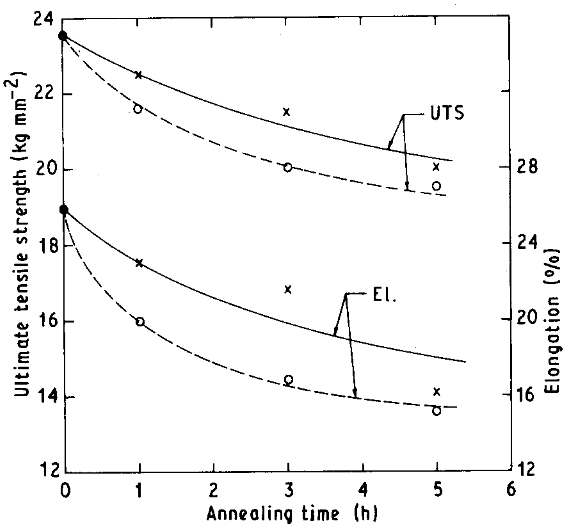

Figure 6 The influence of annealing time on the tensile strength and elongation of the Al–Mg alloy at annealing temperatures of (×) 723 and (o) 773 K.

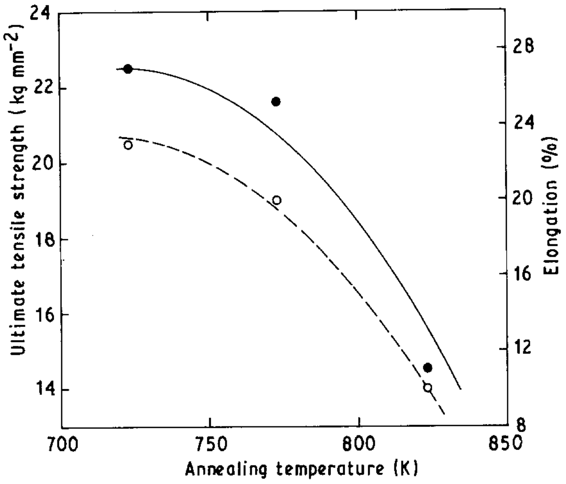

Figure 7 The influence of annealing temperature on (●) the tensile strength and (o) elongation of the Al–Mg alloy for a holding time of 1 h.

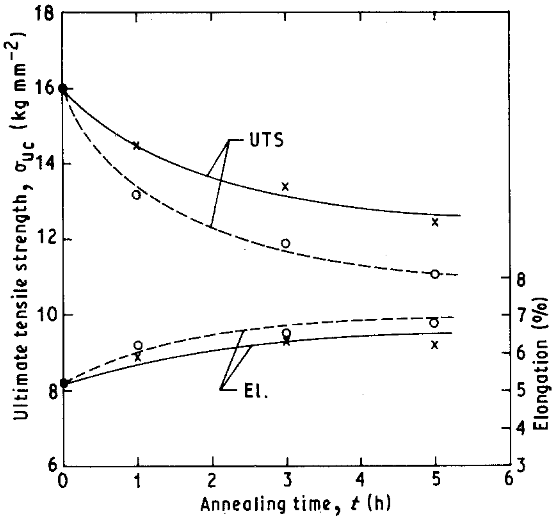

Figure 8 The influence of annealing time on the tensile strength and elongation of the composite at different annealing temperatures of (×) 673 and (o) 723 K.

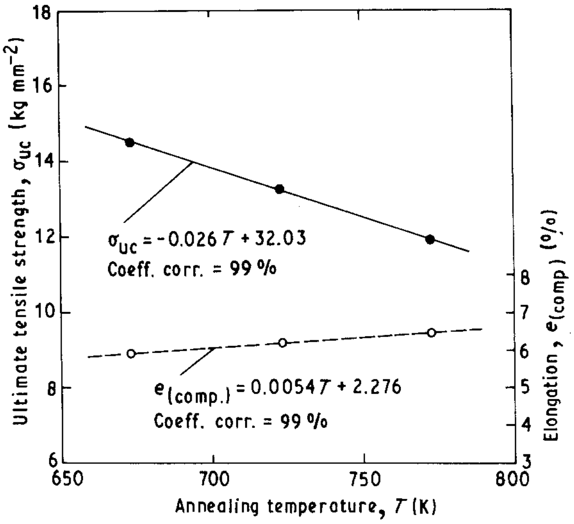

Figure 9 The influence of annealing temperature on (●) the tensile strength and (o) elongation of the composite for a holding time of 1 h.

At a given annealing temperature, T, of 673 or 723 K the influence of annealing time, t, on the ultimate tensile strength, σ_{uc}, and elongation of the composite are shown in Fig. 8. The figure shows that the increase in annealing time up to 5 h enhances the elongation of the composite from about 5.2% in the as-cast composite to about 6.27% and 6.8% at annealing temperatures of 673 and 723 K, respectively. However, an increase in annealing time up to 5 h has been found to reduce the ultimate tensile strength of the composite from about 16.0 kg mm^{-2} in the as-cast composite, to about 12.5 and 11.1 kg mm^{-2} when the composites are annealed at temperatures of 673 and 723 K, respectively. The reduction in UTS of composites with increasing annealing time, t, can be expressed by

$$\sigma_{uc} = -0.0465t + 2.746 \quad \text{at } 673\text{ K} \qquad (1)$$

and

$$\sigma_{uc} = -0.0668t + 2.709 \quad \text{at } 723\text{ K} \qquad (2)$$

having a coefficient of correlation of 97% and 93%, respectively. The results presented in Fig. 8 also show that during annealing for a given time, the increase in annealing temperature reduces the tensile strength and enhances the elongation of the composite. This behaviour is further evident in Fig. 9. It is interesting to note in Figs 6–9 that the increase in annealing time or temperature reduces the elongation of the Al–Mg alloy but enhances it in the composites.

Typical fractographs of the fractured tensile specimens of the as-cast composites and those heat treated at 723 K for 5 h and at 773 K for 1 h, are shown in Fig. 10a–c, respectively. The fractographs show that the materials are fractured in the ductile mode, but the dimples become comparatively larger with annealing, especially when the annealing temperature is kept at 773 K, as shown in Fig. 10c.

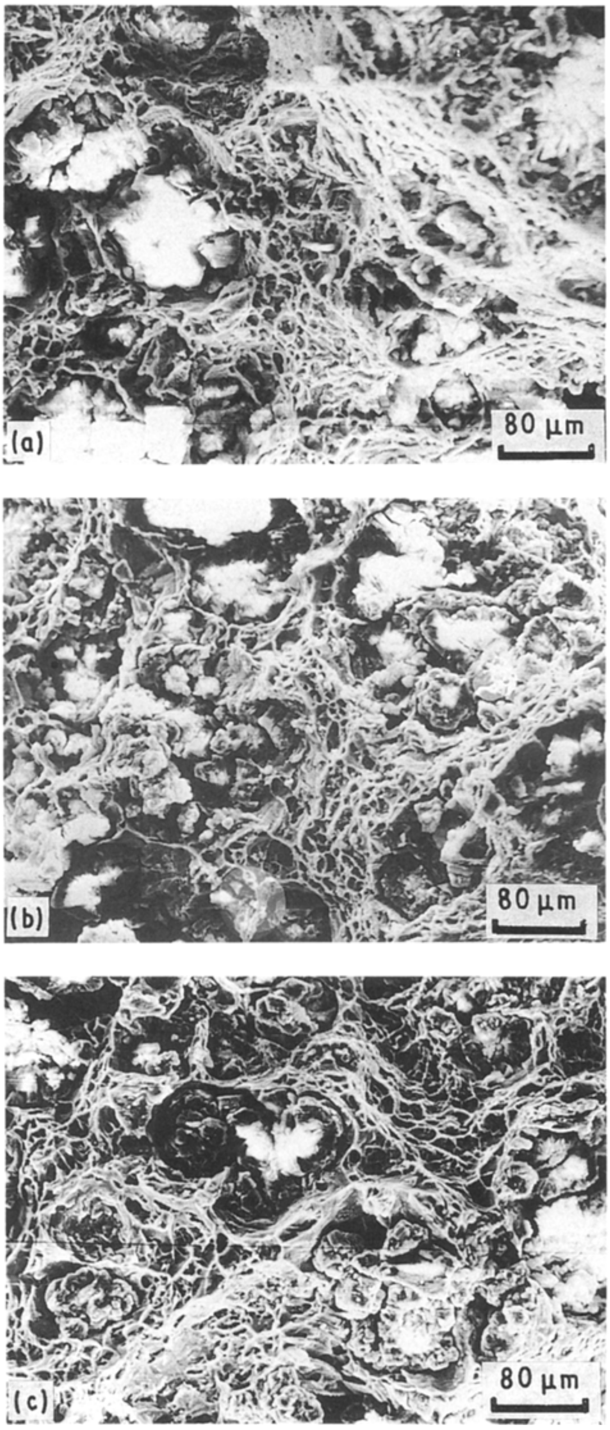

Figure 10 Influence of annealing on the fracture behaviour of the composite: (a) as-cast, (b) annealed at 723 K for 5 h and (c) annealed at 773 K for 1 h.

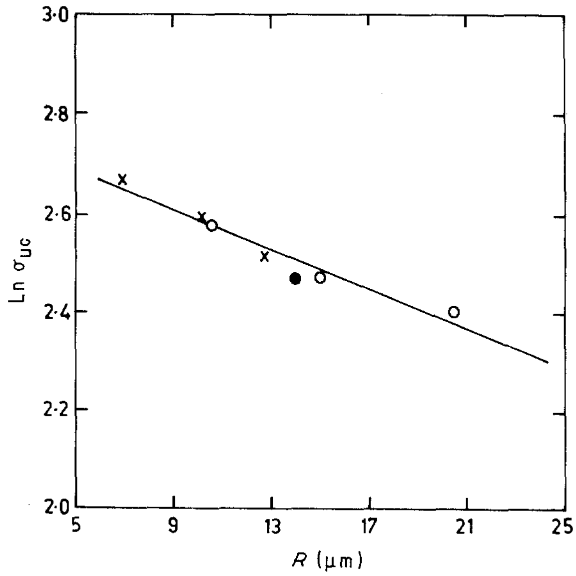

Figure 11 The correlation between the thickness of the reacted layer and the tensile strength of the composite during annealing, at (×) 673 K, (o) 723 K and (●) 773 K.

The influence of thickness of the reacted layer at the particle–matrix interface, on the mechanical properties of the composite is shown in Fig. 11. The figure shows that the increase in thickness of the reacted layer, R, with annealing reduces the ultimate tensile strength of the composite, σ_{uc}, significantly together with a moderate increase in its elongation. The decrease in σ_{uc} with increase in R has been found to follow a linear relationship $\sigma_{uc} = -0.0199R + 2.786$, having a coefficient of correlation of the order of 96%.

4. Discussion

The presence of microcracks in the reacted layer at the particle–matrix interface of as-cast composite (Fig. 3a) has been reported earlier and these cracks may have resulted due to thermal stress developing because of differential thermal contraction during solidification and cooling. However, the reacted layer growing during annealing is relatively free from such cracks because of the absence of such severe thermal stresses, as the sample did not go through solidification and cooling from its relatively high melting temperature, after formation of the reacted layer. Further, the microcrack at the reacted layer of the cast composite may have healed during annealing (Fig. 4a) due to material transport by diffusion and chemical reaction.

The decrease in matrix hardness of the composite (Fig. 4) and the Al–Mg alloy (Fig. 5) with increasing extent of annealing either in temperature or time, is due to the homogenization of the matrix, as revealed in the optical micrographs of the composite shown in Fig. 2a and b. However, at a given temperature and time during annealing, the relatively lower reduction in matrix hardness of the composite compared to that observed in the Al–Mg alloy may have been due to the presence of dispersed particles, which restricts the flow of the matrix and contributes to its hardness.

The mechanical properties of particulate composite are to a great extent dependent on the nature of the dispersed particle–matrix interface and its debonding characteristics. The fractographs in Fig. 10b and c show that in the annealed composite the debonding has taken place primarily along the interface between the matrix and reacted layer on the particle, as observed in the as-cast composites. The reacted layer around the particle is clearly identified by its different charging characteristics under SEM from that of alumina.

The most interesting result of the present investigation is the contrast in the trend of variation of elongation on annealing in Al–Mg alloy and that in Al–Mg alloy-base composites, as shown in Figs 6 and 8. When cast Al–Mg alloy is annealed, the eutectic produced as a result of segregation begins to disappear resulting in increasing magnesium content of the primary phase. The contribution of this phase to the strength increases due to solution hardening but it could not counterbalance the decrease in strength due to the disappearance of the eutectic. Thus, the overall strength of the Al–Mg alloy decreases with extent of annealing, as shown in Figs 6 and 7. The elongation of single-phase Al–Mg alloy is reduced with magnesium content [10] and so, it is not surprising that the elongation of cast Al–Mg alloy is also reduced with annealing, because the magnesium content of the primary phase increases. The contribution of disappearance of the brittle eutectic could not outweigh this effect.

In cast Al–Mg alloy-base composite, the dispersed particles of alumina are often surrounded by the last freezing liquid, transforming sometimes by eutectic solidification. The magnesium-rich areas are around the particles and annealing results in diffusion of magnesium inside the alumina particle and its further reaction to extend the reacted layer inside the particle. Because the magnesium content of the primary phase does not increase due to homogenization and the relatively brittle eutectic started to disappear, the elongation of the composite increased with annealing as shown in Figs 8 and 9. Also, the primary phase in the composite does not have the benefit of solution hardening and so, the strength of the composite decreases with annealing. Fig. 11 shows an excellent correlation between the thickness of the reacted layer and the observed ultimate tensile strength of the composite. This is probably due to the fact that the thickness of the reacted layer is a direct measure of magnesium removal from the matrix alloy and the reduction in strength is a consequence of it. It is believed that Fig. 11 does not indicate any role of the thickening reacted layer in reducing the strength directly.

References

1. P. K. GHOSH, P. R. PRASAD and S. RAY, *Z. Metallkde* **75** (1984).
2. P. K. GHOSH and S. RAY, *J. Mater. Sci.* **21** (1986) 1667.
3. *Idem*, *Ind. J. Tech.* **26** (1988) 83.
4. *Idem*, *J. Mater. Sci.* **22** (1987) 4077.
5. P. K. GHOSH and S. RAY, in "Fabrication of Particulates Reinforced Metal Composites", edited by J. Masounave and F. G. Hamel (ASM International, Metals Park, OH, (1990) p. 23.
6. C. G. LEVI, G. J. ABBASCHIAN and R. MEHRABIAN, *Met. Trans.* **9A** (1978) 697.
7. P. K. GHOSH and S. RAY, *Z. Metallkde* **81** (1990) 525.
8. P. K. GHOSH, S. RAY and P. K. ROHATGI, *Trans. J. Inst. Met.* **25** (1984) 440.
9. P. K. GHOSH and S. RAY, *AFS Trans.* **88** (1988) 775.
10. J. E. HATCH (ed.), "Aluminum", (ASM International, Metals Park, OH, 1984) p. 213.

Received 29 January
and accepted 6 July 1992